

## Supporting Information

### **High-brightness green InP-based QLEDs enabled by in-situ passivating core surface with zinc myristate**

Yuanbin Cheng†, Qian Li†, Mengyuan Chen, Fei Chen\*, Zhenghui Wu\* and Huaibin Shen

†*These authors contributed equally to this work.*

Key Laboratory for Special Functional Materials of Ministry of Education, National & Local Joint Engineering Research Center for High-efficiency Display and Lighting Technology

Henan University, Kaifeng 475004, China

E-mail: [chenfei.henu@henu.edu.cn](mailto:chenfei.henu@henu.edu.cn) and [wuzhenghuihk@henu.edu.cn](mailto:wuzhenghuihk@henu.edu.cn)

## ***Chemicals***

Zinc acetate ( $\text{Zn}(\text{Ac})_2$ , 99.99%), indium acetate ( $\text{In}(\text{Ac})_3$ , 99.99%), selenium (Se, 99.99%, powder), myristic acid (MA, 99%), sulfur (S, 99.5%, powder), zinc stearate ( $\text{Zn}(\text{St})_2$ , 12.5~14.0% ZnO), trioctylphosphine (TOP, 97%),  $(\text{TMS})_3\text{P}$  (98%), and 1-octadecene (ODE, 90%), tetramethylammonium hydroxide (TMAH, 99%), magnesium acetate tetrahydrate ( $\text{Mg}(\text{OAc})_2 \cdot 4\text{H}_2\text{O}$ , 99.98%), zinc(II) acetate dihydrate ( $\text{Zn}(\text{OAc})_2 \cdot 2\text{H}_2\text{O}$ , 99.99%) were purchased from Shanghai Aldrich Reagent Company. Poly((9,9-dioctylfluorenyl-2,7-diyl)-alt-(9-(2-ethylhexyl)-carbazole-3,6-diyl)) (PF8Cz,  $\text{MW} \approx 80000$ ) were purchased from volt-amp optoelectronics tech. co., LTD. Ethyl alcohol (HPLC) and dimethyl sulfoxide (DMSO, 99.7%) were provided by Acros Reagent Company. Chlorobenzene, n-octane, hexanes, and ethanol were purchased from Beijing Chemical Reagent Ltd., China.

## ***Preparation of precursors***

Phosphorus precursors: 0.14 mmol of  $(\text{TMS})_3\text{P}$  was mixed in 1 mL of TOP.

Se precursors (Se-ODE): 2 mmol of Se was dissolved in 10 mL of ODE. The concentration is  $0.2 \text{ mol L}^{-1}$ .

S precursors (S-TOP-ODE): 5 mmol of S was dissolved in 5 mL of TOP and 5 mL ODE. The concentration is  $0.5 \text{ mol L}^{-1}$ .

ZnMy<sub>2</sub> precursors: the mixture of 1.25 mmol  $\text{Zn}(\text{Ac})_2$ , 1.25 mmol MA and 10 mL ODE was degassed at  $150 \text{ }^\circ\text{C}$  for 30 min, and then cooled to  $100 \text{ }^\circ\text{C}$  and stored in an  $\text{N}_2$ -filled flask.

## ***Device fabrication***

The indium tin oxide (ITO) glass substrates were thoroughly cleaned with deionized water, acetone, and isopropanol, respectively, and then treated under UV-ozone for 15 min. For the hole injection layer (HIL), poly(3,4-ethyle nedioxythiophene):polystyrenesulfonate (PEDOT:PSS) (AI 4083) was spin-coated onto the ITO substrates and annealed at  $140 \text{ }^\circ\text{C}$  for 15 min. Then, these substrates were swiftly transferred into nitrogen-filled glove box for spin-coating the following layer. PF8Cz ( $8 \text{ mg mL}^{-1}$  in chlorobenzene) was spin-coated and annealed at  $150 \text{ }^\circ\text{C}$  for 30 min for use as hole transport layer (HTL) material. In turn, InP/ZnSe/ZnS ( $20 \text{ mg mL}^{-1}$  in n-octane) and ZnMgO ( $30 \text{ mg mL}^{-1}$  in ethanol, were spin-coated at 2000 and 2500 rpm for 20 s, respectively, and followed by baking at  $60 \text{ }^\circ\text{C}$  for 30 min. Finally, an Al anode was deposited via thermal evaporation under a high vacuum of  $4 \times 10^{-6}$  Torr, and the effective area is  $4 \text{ mm}^2$ .

## ***Materials and devices characterization***

UV-vis absorption and photoluminescence (PL) spectra were measured by Ocean Optics spectrophotometer (model PC2000-ISA). X-ray photoelectron spectroscopy (XPS) was recorded by a

VG ESCALAB 220i-XL spectrometer with a 300 W Al K $\alpha$  radiation source, and all binding energies for different elements were calibrated with respect to the C 1s line at 284.8 eV. PL QY data was collected by JY HORIBA FluoroLog-3 fluorescence spectrometer coupled with an integrating sphere. A JEOL JEM-2010 electron microscope operating at 200 kV was used to obtain transmission electron microscopy (TEM) studies. X-ray diffraction (XRD) patterns were recorded on a Bruker D8 Advance diffraction meter using a Cu K $\alpha$  radiation source ( $\lambda = 1.54056 \text{ \AA}$ ). An Edinburgh F900 steady/transient state fluorescence spectrometer was used to record the time-resolved PL spectra. The current density-luminance-voltage (J-L-V) characteristics of QLEDs were analyzed using an Agilent 4155C semiconductor parameter analyzer with a calibrated Newport silicon diode. The combination of an Ocean Optics (USB 2000) spectrometer and a Keithley 2400 source meter was used to record the EL spectra. All the measurements were performed at room temperature.

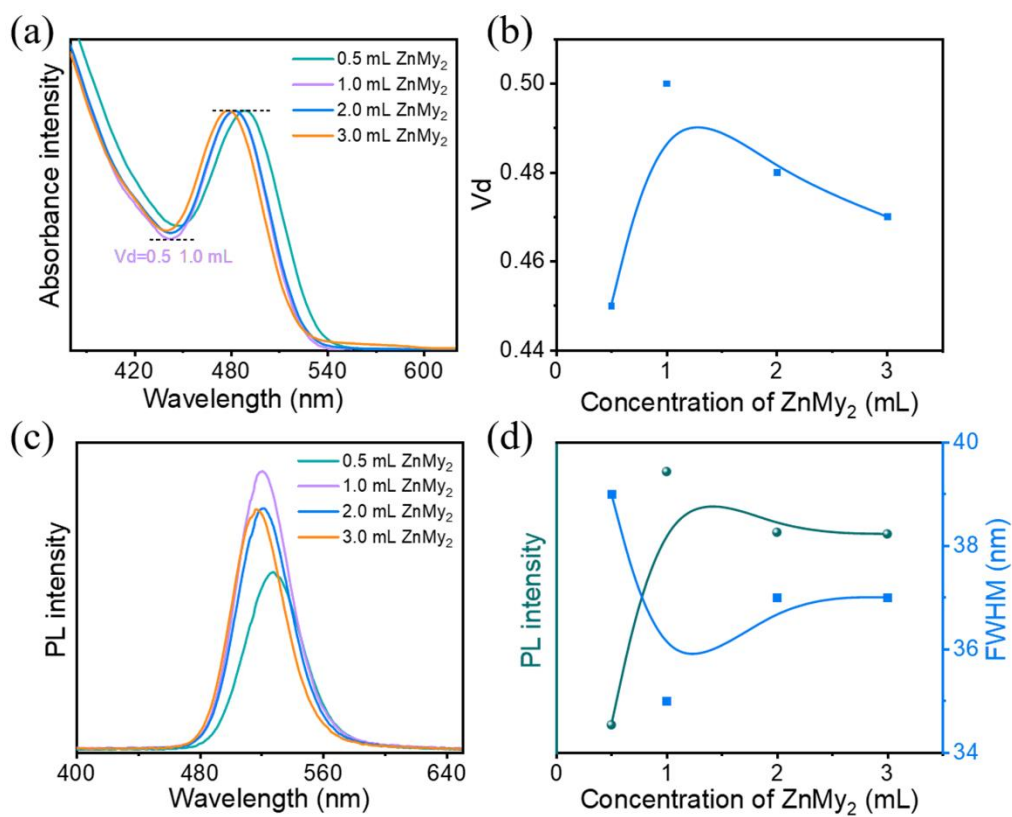


**Figure S1.** (a) UV-vis absorption spectra of InP cores with ZnMy<sub>2</sub> at different concentration. (b) Vd as a function of ZnMy<sub>2</sub> concentration. (c) PL spectra of InP cores with ZnMy<sub>2</sub> at different concentration. (d) PL intensity and FWHM as a function of ZnMy<sub>2</sub> concentration.

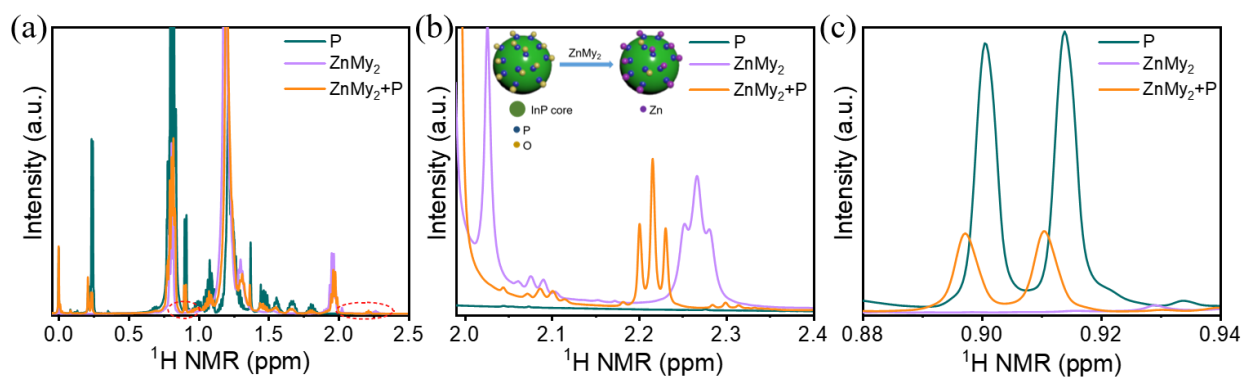


**Figure S2.**  $^1\text{H}$  NMR spectra of phosphorus precursors,  $\text{ZnMy}_2$  and the mixture of phosphorus precursors and  $\text{ZnMy}_2$  in chloroform-d. Inset is the schematic illustration of the  $\text{ZnMy}_2$ -treated InP core.

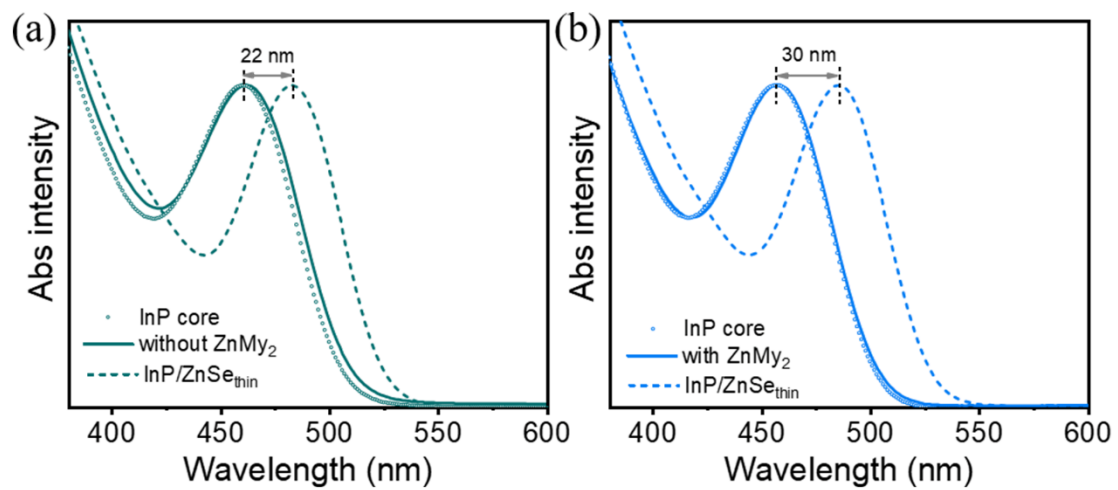


**Figure S3.** UV-vis absorption spectra of InP/ZnSe<sub>thin</sub> cores (a) without and (b) with ZnMy<sub>2</sub>.

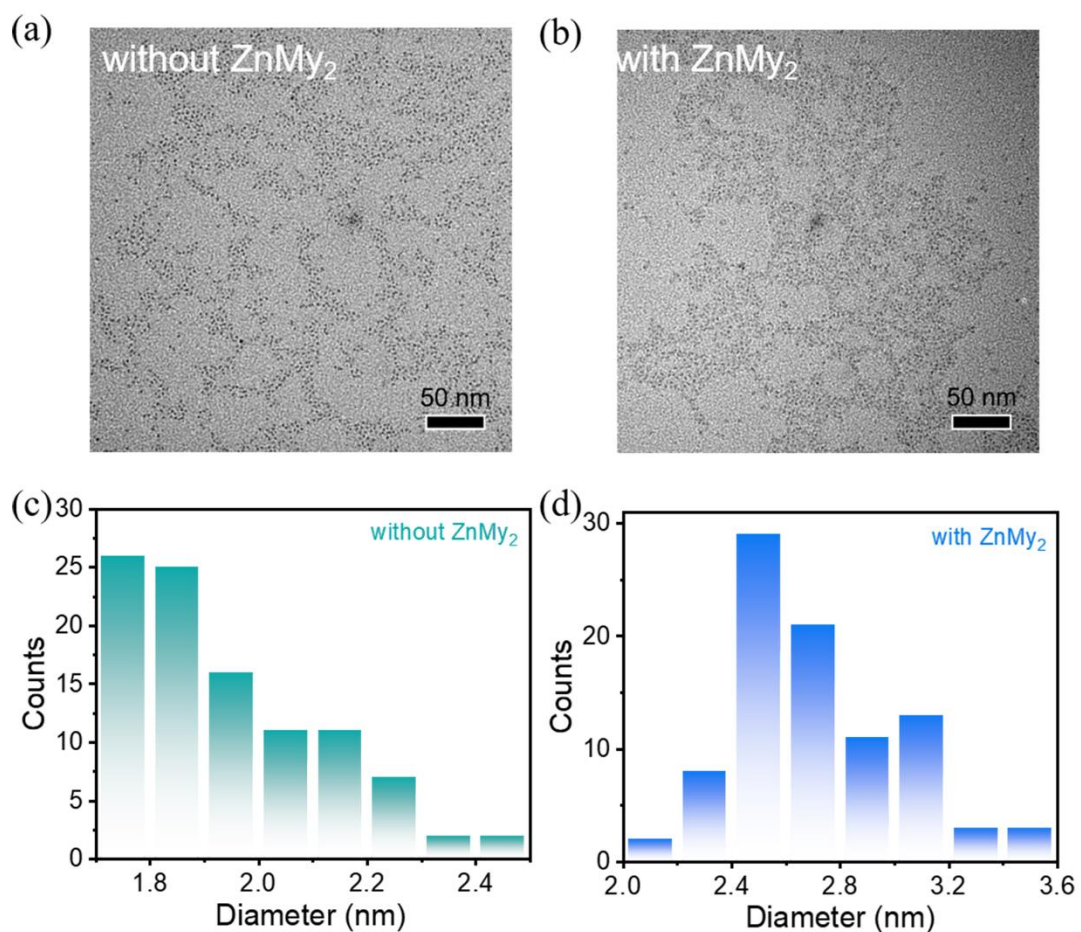


**Figure S4.** TEM pictures of InP/ZnSe<sub>thin</sub> core synthesized (a) without and (b) with ZnMy<sub>2</sub>. The corresponding size distribution histograms of InP/ZnSe<sub>thin</sub> cores synthesized (c) without and (d) with ZnMy<sub>2</sub>.

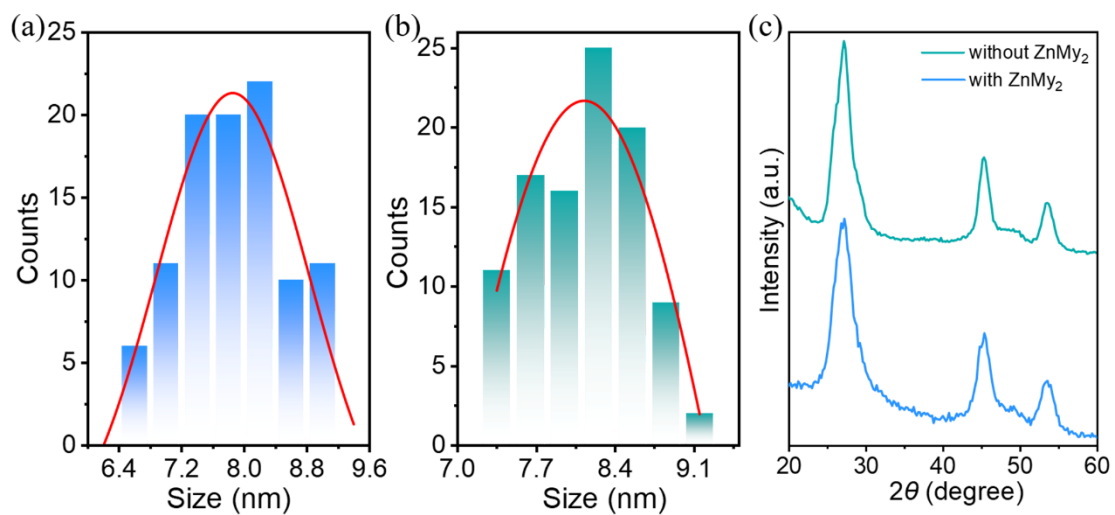


**Figure S5.** Size distribution histograms of InP/ZnSe/ZnS QDs synthesized (a) without and (b) with ZnMy<sub>2</sub>. (c) The corresponding XRD patterns.



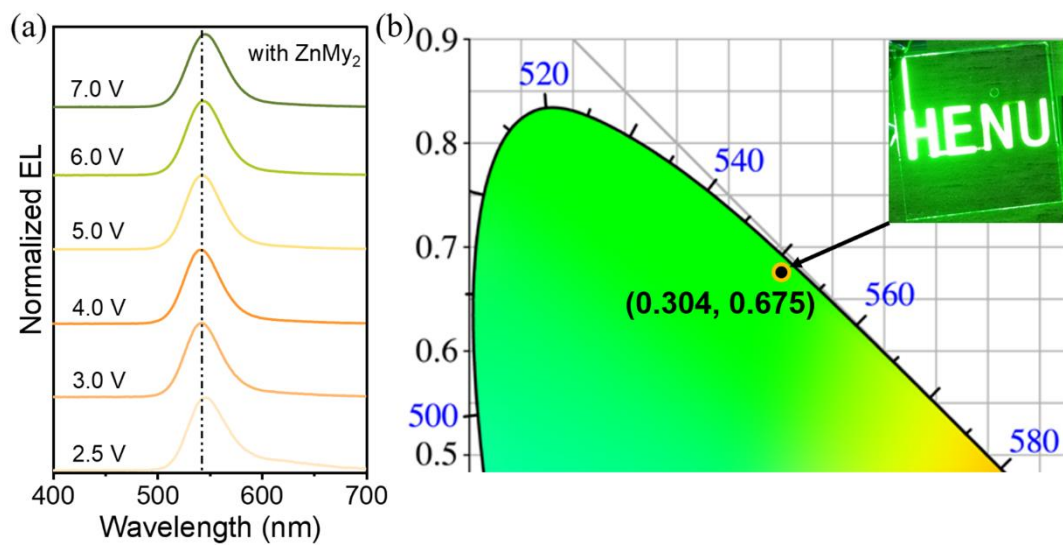


**Figure S6.** (a) Electroluminescence (EL) spectra of QLEDs under different driving voltages. (b) CIE chromatic coordinates of our QLED, and the inset shows the photograph of EL emission from the device operated at 5 V.

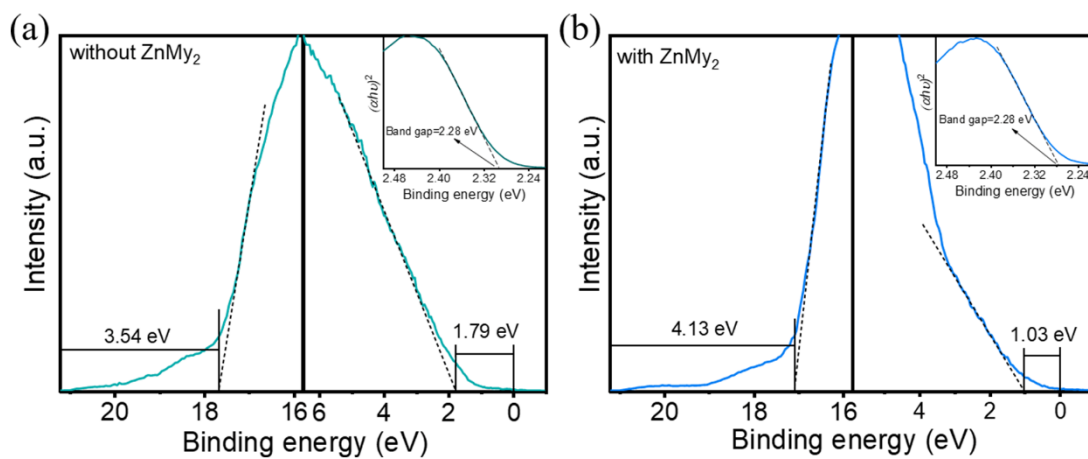


**Figure S7.** The ultraviolet photoelectron spectroscopy (UPS) spectra of the high-binding energy secondary electron cutoff regions and the valence-band edge regions of InP/ZnSe/ZnS QDs synthesized (a) without and (b) with ZnMy<sub>2</sub>.

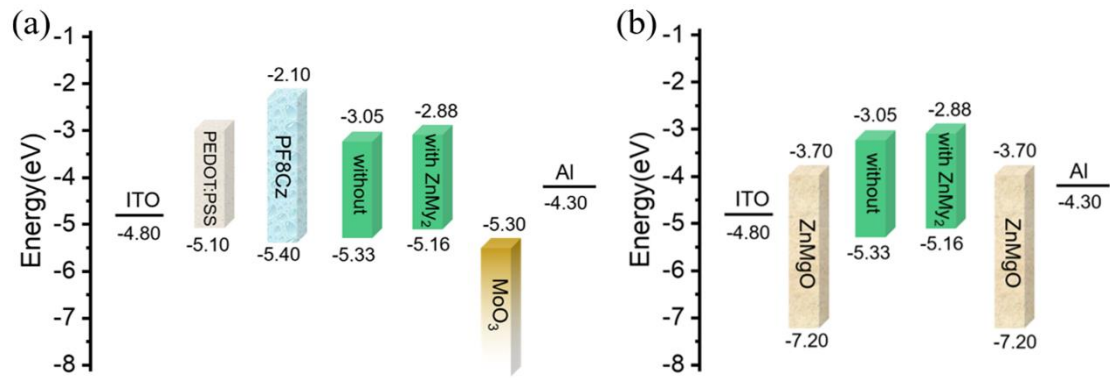


**Figure S8.** Energy level diagrams of (a) HOD with ITO/PEDOT:PSS/TFB/QDs/MoO<sub>3</sub>/Al and (b) EOD with ITO/ZnMgO/QDs/ZnMgO/Al.

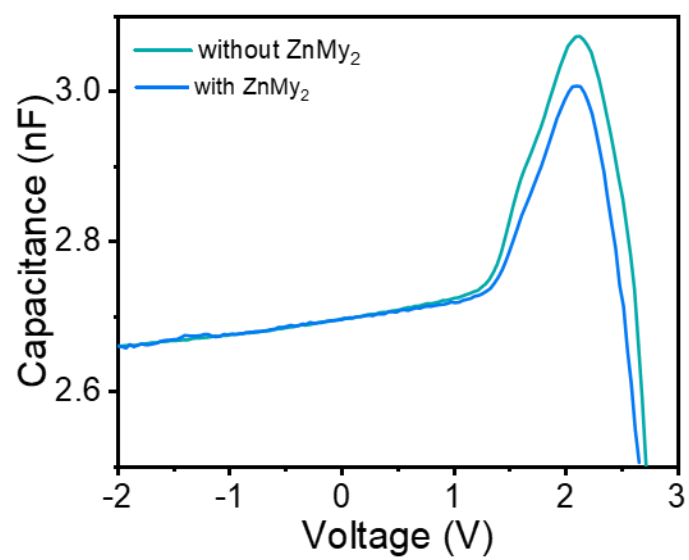


**Figure S9.** The capacitance-voltage characteristics of QLEDs based on InP/ZnSe/ZnS QDs synthesized without and with ZnMy<sub>2</sub>.

**Table S1.** Comparison of the device performance in this work and from other works reported previously.

Year	PL (nm)	FWHM (nm)	PL QY (%)	Device structure	EQE (%)	$\eta_A$ (cd A <sup>-1</sup> )	L (cd m <sup>-2</sup> )	Von (V)	T <sub>50@100</sub> cd m <sup>-2</sup> (h)	Ref.
2013	518	64	80	ITO/ZnO/PFN/InP@ZnSeS/TC TA/MoO <sub>3</sub> /Al	3.46	10.9	3900	2.2		1
2019	516	53	67	ITO/PEDOT:PSS/TFB/InP/GaP/ZnS/ZnO/Al	6.3	13.7	2938	2.6		2
2019	531	34	82	ITO/PEDOT:PSS/poly-TPD:PVK/InP QD/ZnMgO/Al	13.6		13900	2.5		3
2019	529	41	86	Glass/Ag/ZnO/PFN/InP/ZnSeS/CzSi/TCTA/MoO <sub>x</sub> /Ag		15.3	38800			4
2020	525	40	81	ITO/ZnO/TmPPPyTz/InP QD/TCTA/MoO <sub>3</sub> /Al	10			2.4		5
2021	545		86	ITO/ZnMgO/InP/ZnSe/ZnS/TC TA/MoO <sub>3</sub> /Al	16.3	57.5	12646.3	2	1033.4	6
2022	526	35	97	ITO/PEDOT:PSS/TFB/InP QD/ZnSe <sub>x</sub> S <sub>1-x</sub> /ZnS/ZnMgO/Al	15.2		2300@4V	2.1		7
2022	535	43	54	ITO/PEDOT:PSS/PVK/InP/ZnSe/ZnS/PO-T2T/Al	15		10010	3.1	1430	8
2022	528	38	89	ITO/ZnO@ZnS/In(Zn)P/ZnSeS/ZnS/DBTA/PCBBiF/HATCN/Al	10.8	37.5	1756	2.4	60255	9
2022	510	36	91	ITO/PEDOT:PSS/TFB/PVP/InP/ZnSe/ZnS/ZnO/Al	10.6	40.7	15606	1.8	5642	10
2023	533			ITO/PEDOT:PSS/MoO <sub>3</sub> /PVK/InP/ZnS/ZnO/Al	7.39		52730	2.5	104.09	11
2023	529		80	Ag/ZnMgO/InP/ZnSe/ZnS/TA DF-EHL/TCTA/MoO <sub>3</sub> /Ag		68	40700			12
2023	532	36	90	ITO/PEDOT:PSS/PTAA/InP/ZnSe/ZnS/ZnMgO@NaCl/Al	13.8	52.2	16788	2.2	5944	13
2023	535	33.7	95	ITO/PEDOT:PSS/TFB/InP/ZnSeS/ZnS/ZnMgO/Al	14.3	39	11920	2.2		14
2024	534	44	91	ITO/PEDOT:PSS/PF8Cz/InP/ZnSe/ZnS/ZnMgO/Al	12.74	53.31	175084	2.0	20044	This work

## Supplementary References

- [1] Lim J, Park M, Bae W K, Lee D, Lee S, Lee C and Char K 2013 Highly Efficient Cadmium-Free Quantum Dot Light-Emitting Diodes Enabled by the Direct Formation of Excitons within InP@ZnSeS Quantum Dots *ACS Nano* **7**, 9019-9026.

- [2] Zhang H, Hu N, Zeng Z, Lin Q, Zhang F, Tang A, Jia Y, Li L S, Shen H, Teng F and Du Z 2019 High-Efficiency Green InP Quantum Dot-Based Electroluminescent Device Comprising Thick-Shell Quantum Dots *Adv. Optical Mater.* **7**, 1801602.
- [3] Moon H, Lee W, Kim J, Lee D, Cha S, Shin S and Chae H 2019 Composition-tailored ZnMgO nanoparticles for electron transport layers of highly efficient and bright InP-based quantum dot light emitting diodes *Chem. Commun.* **55**, 13299-13302.
- [4] Lee T, Hahm D, Kim K, Bae W K, Lee C, and Kwak J 2019 Highly Efficient and Bright Inverted Top-Emitting InP Quantum Dot Light-Emitting Diodes Introducing a Hole-Suppressing Interlayer *Small* **15**, 1905162.
- [5] Iwasaki Y, Motomura G, Ogura K, and Tsuzuki T 2020 Efficient green InP quantum dot light-emitting diodes using suitable organic electron-transporting materials *Appl. Phys. Lett.* **117**, 111104.
- [6] Chao W C, Chiang T H, Liu Y C, Huang Z X, Liao C C, Chu C H, Wang C H, Tseng H W, Hung W Y and Chou P T 2021 High efficiency green InP quantum dot light-emitting diodes by balancing electron and hole mobility *Commun. Mater.* **2**, 96.
- [7] Yu P, Cao S, Shan Y, Bi Y, Hu Y, Zeng R, Zou B, Wang Y and Zhao J 2022 Highly efficient green InP-based quantum dot light-emitting diodes regulated by inner alloyed shell component *Light: Sci. Appl.* **11**, 162.
- [8] Gao P, Zhang Y, Qi P, and Chen S 2022 Efficient InP Green Quantum-Dot Light-Emitting Diodes Based on Organic Electron Transport Layer *Adv. Optical Mater.* **10**, 2202066.
- [9] Mude N N, Khan Y, Thuy T T, Walker B and Kwon J H 2022 Stable ZnS Electron Transport Layer for High-Performance Inverted Cadmium-Free Quantum Dot Light-Emitting Diodes *ACS Appl. Mater. Interfaces* **14**, 5592555932.
- [10] Wu Q, Cao F, Wang S, Wang Y, Sun Z, Feng J, Liu Y, Wang L, Cao Q, Li Y, Wei B Wong W Y, and Yang X 2022 Quasi-Shell-Growth Strategy Achieves Stable and Efficient Green InP Quantum Dot Light-Emitting Diodes *Adv. Sci.* **9**, 2200959.
- [11] Zhang T, Liu P, Zhao F, Tan Y, Sun J, Xiao X, Wang Z, Wang Q, Zheng F, Sun X W, Wu D, Xing G and Wang K 2023 Electric dipole modulation for boosting carrier recombination in green InP QLEDs under strong electron injection *Nanoscale Adv.* **5**, 385.
- [12] Kim J, Hong A, Hahm D, Lee H, Bae W K, Lee T and Kwak J 2023 Realization of Highly Efficient InP Quantum Dot Light-Emitting Diodes through In-Depth Investigation of Exciton-Harvesting Layers *Adv. Optical Mater.* **11**, 2300088.
- [13] Wu Q, Wang L, Cao F, Wang S, Li L, Jia G and Yang X 2023 Bridging Chloride Anions Enables Efficient and Stable InP Green Quantum-Dot Light-Emitting Diodes *Adv. Optical Mater.* **11**, 2300659.
- [14] Shin S, Gwak N, Yoo H, Jang H, Lee M, Kang K, Kim S, Yeon S, Kim T A, Kim S, Hwang G W and Oh N 2023 Fluoride-free synthesis strategy for luminescent InP cores and effective shelling processes via combinational precursor chemistry *Chem. Eng. J.* **466**, 143223.